

# Optics Letters

## Step-scan differential Fourier transform infrared photoacoustic spectroscopy (DFTIR-PAS): a spectral deconvolution method for weak absorber detection in the presence of strongly overlapping background absorptions

LIXIAN LIU,<sup>1,2</sup> ANDREAS MANDELIS,<sup>1,2,\*</sup> HUITING HUAN,<sup>1,2</sup> AND KIRK H. MICHAELIAN<sup>2,3</sup>

<sup>1</sup>School of Optoelectronic Information, University of Electronic Science and Technology of China, Chengdu 610054, China

<sup>2</sup>Center for Advanced Diffusion-Wave and Photoacoustic Technologies (CADIPT), Department of Mechanical and Industrial Engineering, University of Toronto, Toronto, Ontario M5S 3G8, Canada

<sup>3</sup>CanmetENERGY, Natural Resources Canada, Devon, Alberta T9G 1A8, Canada

\*Corresponding author: mandelis@mie.utoronto.ca

Received 16 January 2017; revised 18 February 2017; accepted 19 February 2017; posted 13 March 2017 (Doc. ID 284787); published 30 March 2017

The determination of small absorption coefficients of trace gases in the atmosphere constitutes a challenge for analytical air contaminant measurements, especially in the presence of strongly absorbing backgrounds. A step-scan differential Fourier transform infrared photoacoustic spectroscopy (DFTIR-PAS) method was developed to suppress the coherent external noise and spurious photoacoustic (PA) signals caused by strongly absorbing backgrounds. The infrared absorption spectra of acetylene ( $C_2H_2$ ) and local air were used to verify the performance of the step-scan DFTIR-PAS method. A linear amplitude response to  $C_2H_2$  concentrations from 100 to 5000 ppmv was observed, leading to a theoretical detection limit of 5 ppmv. The differential mode was capable of eliminating the coherent noise and dominant background gas signals, thereby revealing the presence of the otherwise hidden  $C_2H_2$  weak absorption. Thus, the step-scan DFTIR-PAS modality was demonstrated to be an effective approach for monitoring weakly absorbing gases with absorption bands overlapped by strongly absorbing background species. © 2017 Optical Society of America

**OCIS codes:** (010.1120) Air pollution monitoring; (070.0070) Fourier optics and signal processing; (300.0300) Spectroscopy; (040.3060) Infrared; (300.6300) Spectroscopy, Fourier transforms.

<https://doi.org/10.1364/OL.42.001424>

Gas phase photoacoustic spectroscopy (PAS) is widely applied for trace contaminant monitoring, due to its high resolution, large dynamic range, and simple experimental setup [1]. The sensitivity of the PAS method has been improved by acoustic signal amplification produced by different resonant cells [2,3] and high incident intensity laser sources [4]. Nevertheless,

problems persist with the methodologies in the presence of strongly absorbing background gases which tend to mask overlapping spectrum signals from weakly absorbing trace gases and vapors such as ambient air contaminants. In this Letter, we present a highly selective broadband detection configuration: a DFTIR-PAS system capable of deconvolving spectra of such weakly absorbing components within an overwhelming strongly absorbing background. We chose  $C_2H_2$  as the case study target gas because its detection is of importance in environmental monitoring and industrial safety operations [5]; some  $C_2H_2$  absorption peaks (around  $1360\text{ cm}^{-1}$ ) are hidden behind the usually much stronger ambient water vapor absorption bands.

The step-scan DFTIR-PAS configuration based on a FTIR spectrometer (Bruker, Vertex 70) is shown in Fig. 1. A chopper with a homemade one-side-coated high-reflectivity blade was used to maximize the incident light energy utilization efficiency, avoiding the need for a beam splitter. Two identical T-resonators [6,7] were introduced to suppress coherent noise and cancel background gas signals by means of out-of-phase

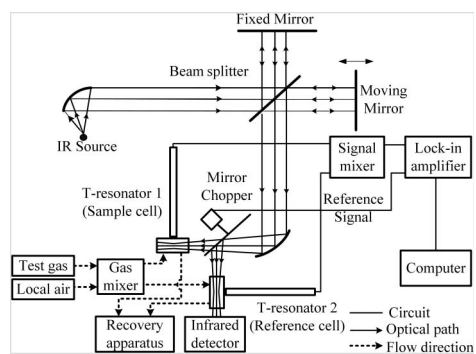


**Fig. 1.** Schematic of the step-scan DFTIR-PAS configuration.

light modulation [8]. A series of  $C_2H_2$  concentrations was premixed with local air in the gas mixer before being admitted into the resonators. The incident light intensity at the target wavenumber was approximately  $30 \mu W$ , as calculated from the intensity distribution of the broadband globar source (total infrared intensity:  $30 mW$ ).

Figure 2(a) shows the single and differential mode step-scan FTIR-PA spectra acquired when the two cells were filled with local laboratory air (relative humidity [RH] about 45%). Both spectra are normalized by the globar source light intensity distribution in the same wavenumber range. The absorption bands (ranges of  $1260\text{--}2000$  and  $3420\text{--}3900 \text{ cm}^{-1}$ ) of the water vapor and the peaks ( $2349 \text{ cm}^{-1}$ ) due to the carbon dioxide are clearly observed in the single mode. These spectral features were significantly suppressed in the differential mode verifying equations (9)–(11) in [8], shown here simplified as Eq. (1):

$$B_D(\sigma_m) = \left[ I(0) + 2 \sum_{j=1}^{N-1} I(jb) \cos(2\pi\sigma_m j b) \right] R_{\text{mic}}(\omega_1) C N_{\text{tot}} \\ \times \left[ E_k(\nu) \sum_{k=1}^T c(k) + \sum_{k'=1}^{T'} c(k') E_{k'}(\nu) (1 + e^{i\varphi}) \right] \\ j: 1, 2, 3 \dots N-1, m: 1, 2, 3 \dots M. \quad (1)$$

$B_D(\sigma_m)$  is the DFTIR-PAS signal as a function of wavenumber  $\sigma_m$  ( $m \in [1, M]$ );  $M$  stands for the number of wavenumbers (ordinates) considered in one spectrum.  $I(jb)$  is the light intensity of the FTIR spectrometer versus optical path difference  $jb$  ( $b$  is the retardation between adjacent sampling points; there are  $N$  sampled points in one interferogram).  $I(0)$  stands for the light intensity at zero retardation.  $R_{\text{mic}}$  is the microphone sensitivity;  $\omega_1$  is the angular modulation angular frequency and is equal to the fundamental resonance angular frequency of the T-cells.  $C$  is the cell constant.  $N_{\text{tot}}$  is the total number density of molecules.  $c(k)$  and  $E_k(\nu)$  are the concentration and the absorption spectrum of the  $k$ -th component, respectively.  $T$  is the total number of gases to be detected, and  $T'$  is the total number of absorbing gaseous species mixed with the residual (background) gas which can generate a spurious photoacoustic signal (e.g., water vapor in ambient air). The phase difference between the outputs of the two cells,  $\varphi$ , is ideally equal to  $\pi$  as a result of the out-of-phase light modulation. Under these conditions, background signals are cancelled, and only the signal from the target gas is present as shown in Eq. (1).

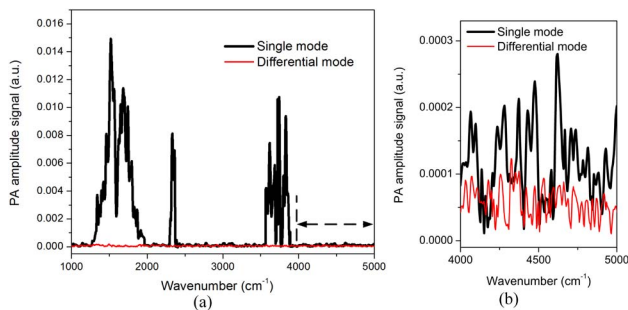


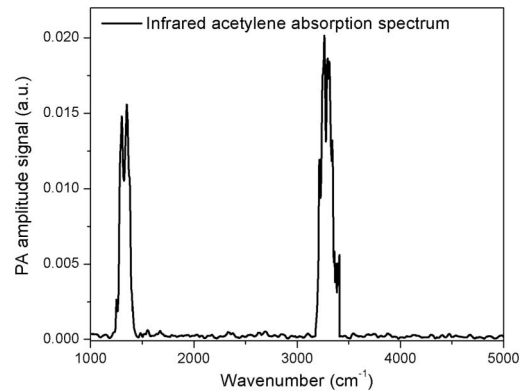
**Fig. 2.** (a) Normalized two-mode step-scan FTIR-PA spectra of laboratory air. (b) Enlargement of the noise floor of the single and differential FTIR-PAS modalities in a selected wavenumber range of (a).

The significant coherent noise attenuation of the differential mode is demonstrated in Fig. 2(b), which is an expanded version of the  $4000\text{--}5000 \text{ cm}^{-1}$  spectrum baseline of Fig. 2(a). It is seen that the single-mode noise level is more than twice as large as that of the differential mode. Figure 2 indicates that the capabilities of the differential mode are twofold: suppression of the coherent noise and cancellation of large background gas/vapor signals. These attributes were found to be the key for the successful deconvolution and emergence of weakly absorbing gas peaks normally “hiding” behind strong absorption spectra of common ambient gases such as water vapor.

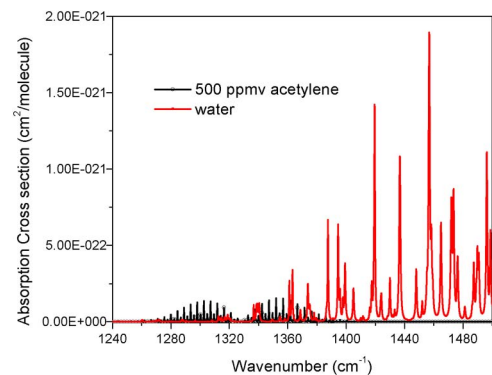
Figure 3 shows the step-scan FTIR-PA  $C_2H_2$  spectrum. Three main peaks are prominent at about  $1302$ ,  $1360$ , and  $3294 \text{ cm}^{-1}$ , respectively. The peaks near  $3294 \text{ cm}^{-1}$  are due to the  $\nu_3$  CH stretching vibration, which is in resonance with the  $\nu_2 + \nu_4 + \nu_5$  combination band [9]. The other two major peaks can be understood as a strong  $\nu_4 + \nu_5$  combination band ( $(\nu_4 + \nu_5)_+$  for  $1308 \text{ cm}^{-1}$  and  $(\nu_4 + \nu_5)_-$  for  $1360 \text{ cm}^{-1}$ ) [10].

Figure 4 shows an overlapping region between the  $C_2H_2$  absorption peaks (around  $1360 \text{ cm}^{-1}$ ) and the water absorption spectrum ( $1300\text{--}1500 \text{ cm}^{-1}$ ) constructed from Hitran data [11]. The water concentration in Fig. 4 was adjusted to be consistent with laboratory air (RH: 45%). The peak intensities of  $500 \text{ ppmv } C_2H_2$  are equivalent to those of the laboratory air water concentration (humidity).

The capability of the step-scan DFTIR-PAS configuration to deconvolute a “hidden” target gas from behind the strong water absorption bands was tested with  $100 \text{ ppmv } C_2H_2$ .



**Fig. 3.** Normalized step-scan FTIR-PA  $C_2H_2$  spectrum.



**Fig. 4.** Absorption cross section of  $C_2H_2$  and water (Hitran data).

The results are shown in Fig. 5. One cell was filled with the mixture of 100 ppmv acetylene and laboratory air, and the other cell contained only laboratory air. The single-mode and differential mode step-scan FTIR-PA spectra of the two cells are shown in Figs. 5(a) and 5(b), respectively. There is no measurable difference between the two spectra in Fig. 5(a) near  $1360\text{ cm}^{-1}$ , which leads to the conclusion that it is difficult or impossible for the single mode to detect 100 ppmv acetylene in the presence of other absorbing species. However, the  $\text{C}_2\text{H}_2$  peaks at  $1308$  and  $1360\text{ cm}^{-1}$  are obviously well distinguished in Fig. 5(b). The differential PA signal strength due to the  $\text{C}_2\text{H}_2$  peak at  $1360\text{ cm}^{-1}$  was  $6.75 \times 10^{-4}$  (arbitrary units, A.U.). The peak signal generated by the target gas is undetectable when it is smaller than the signal fluctuation at baseline (no absorption) which can be taken as the noise floor of the differential mode system. To calculate the fluctuation level, a straight line was fitted to the spectrum in the region where no gas absorption occurs ( $2800\text{--}3050\text{ cm}^{-1}$ ). The standard deviation (fluctuation) between the best-fit straight line and the experimental data was found to be  $3.06 \times 10^{-5}$  (A.U.) and was considered to be the noise floor of the DFTIR-PAS system [8]. The quotient of these values yields a signal-to-noise ratio (SNR) of 22.06 for 100 ppmv  $\text{C}_2\text{H}_2$  by means of DFTIR-PAS, leading to a  $\text{C}_2\text{H}_2$  detection limit of roughly 5 ppmv ( $100/22.06$ ). Scaling to equivalent incident light intensity, the DFTIR-PAS revealed better performance and lower  $\text{C}_2\text{H}_2$  detection limit than several other laser photoacoustic methodologies, as shown in Table 1. Figure 5(c) shows the concentration dependence of the signal amplitudes at the  $\text{C}_2\text{H}_2$  absorption peaks ( $1360\text{ cm}^{-1}$ ) from 5000 to 100 ppmv measured with the step-scan DFTIR-PAS setup. The lower limit of quantification is 17 ppmv using the criterion of acceptable SNR as 10:1. The experimental data show an excellent linear dependence on concentration, which demonstrates that the DFTIR-PAS modality is an effective approach for revealing the presence of “hidden” gases, the absorption peaks of which are concealed due to an overlap with other strongly absorbing background gases.

The “hidden gas” detection capability of a T-cell resonator-enhanced step-scan DFTIR-PAS system was demonstrated by monitoring  $\text{C}_2\text{H}_2$  concentrations mixed with local laboratory air, where strong water absorption bands due to the ambient air strongly dominate the gas mixture spectrum. The linear amplitude response to acetylene concentrations is practical and valuable as it obviates the need for complicated nonlinear calibration algorithms.

In conclusion, by virtue of efficient noise level suppression and differential spectra cancellation, the step-scan T-cell resonator DFTIR-PAS approach was demonstrated to be a sensitive, broadband, quantitative spectroscopic technique for

**Table 1. Summary of Acetylene Detection Limit by Laser Photoacoustic Related Methodologies**

Wavelength (nm)	Absorption Coefficient ( $\text{cm}^{-1}$ )	Incident Light		Detection Limit
		Intensity (mW)		
1530.7	$2.04 \times 10^{-2}$	500		1.56 ppb [12]
1534.099	$3.16 \times 10^{-2}$	1.71		1.5 ppmv [13]
1513.0–1513.3	$5.06 \times 10^{-2}$	3.5		10 ppmv [14]
1529.18	$1.26 \times 10^{-2}$	500		2 ppb [15]

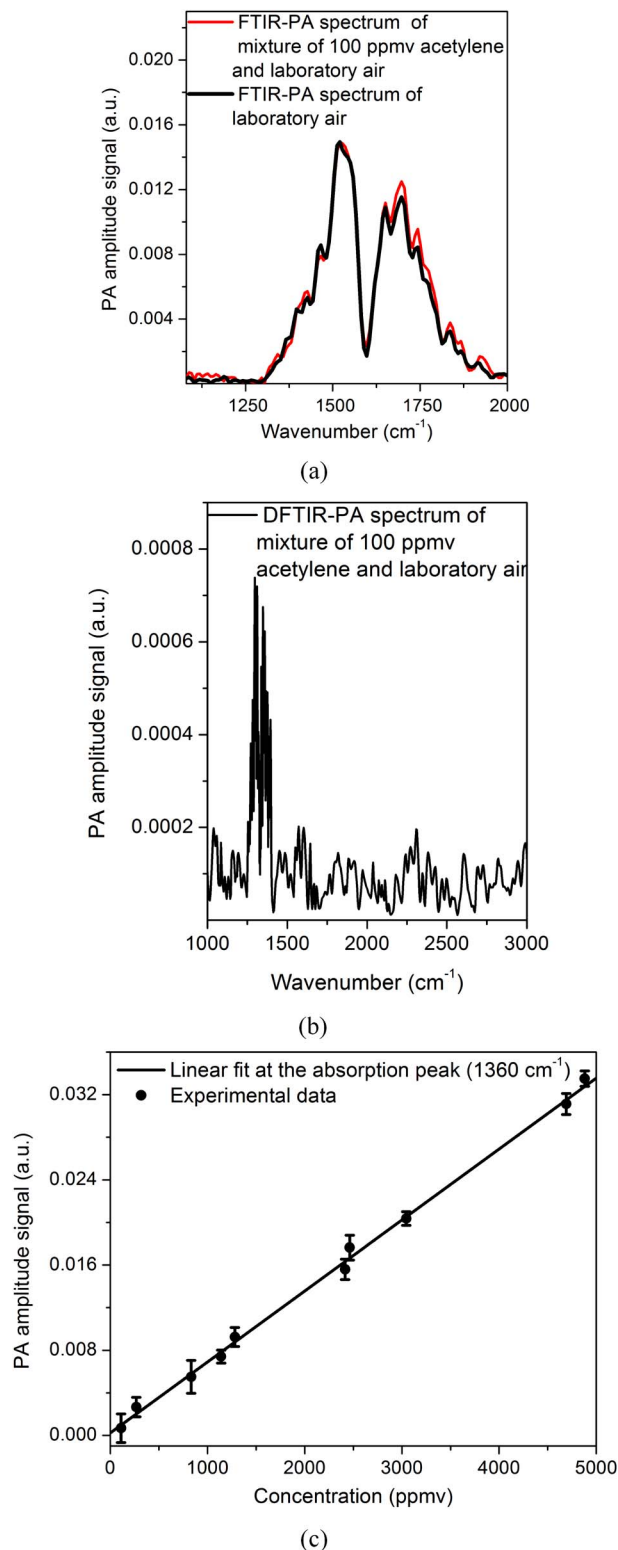


**Fig. 5.** (a) Single-mode step-scan FTIR-PA spectra of the two cells. (One cell is filled with the mixture of 100 ppmv acetylene and laboratory air; the other cell contained laboratory air only.) (b) Step-scan DFTIR-PA spectrum of 100 ppmv  $\text{C}_2\text{H}_2$  and laboratory air. (c) Step-scan DFTIR-PAS amplitude responses at the  $\text{C}_2\text{H}_2$  absorption peak (around  $1360\text{ cm}^{-1}$ ).

ambient trace gas detection in the presence of strongly overlapping absorption bands.

**Funding.** Natural Sciences and Engineering Research Council of Canada (NSERC); National Natural Science Foundation of China (NSFC) (61421002); NNSFC (61574030); China Scholarship Council (CSC).

**Acknowledgment.** The authors are grateful to the Natural Sciences and Engineering Research Council of Canada (NSERC) for a Discovery Grant to A. Mandelis, and to the Canada Research Chairs program. A. Mandelis gratefully acknowledges the Chinese Recruitment Program of Global Experts (Thousand Talents). He also acknowledges the Foundation for Innovative Research Groups of the National Natural Science Foundation of China. L. Liu and H. Huan gratefully acknowledge NNSFC and the China Scholarship Council (CSC) program for an international student grant.

## REFERENCES

1. K. H. Michaelian, *Photoacoustic IR Spectroscopy: Instrumentation, Application and Data Analysis*, 2nd ed. (Wiley, 2010).
2. J. Li, W. Chen, and B. Yu, *Appl. Spectrosc. Rev.* **46**, 440 (2011).
3. J.-P. Besson, S. Schilt, E. Rochat, and L. Thevenaz, *Appl. Phys. B* **85**, 323 (2006).
4. A. Elia, P. M. Lugarà, C. Di Franco, and V. Spagnolo, *Sensors* **9**, 9616 (2009).
5. E. B. Ley and F. J. Vintinner, *Ind. Med. Surg.* **4**, 779 (1945).
6. L. Liu, A. Mandelis, H. Huan, K. Michaelian, and A. Melnikov, *Vib. Spectrosc.* **87**, 94 (2016).
7. L. Liu, A. Mandelis, A. Melnikov, K. Michaelian, and H. Huan, *Int. J. Thermophys.* **103**, 1 (2016).
8. L. Liu, A. Mandelis, H. Huan, and A. Melnikov, *Appl. Phys. B* **122**, 268 (2016).
9. M. Nikow, M. J. Eilhelm, J. M. Smith, and H. Dai, *Phys. Chem. Chem. Phys.* **12**, 2915 (2010).
10. G. Herzberg, *Molecular Spectra and Molecular Structure* (Van Nostrand, 1950).
11. L. S. Rothman, D. Jacquemart, A. Barbe, D. Chris Benner, M. Birk, L. R. Brown, M. R. Carleer, C. Chackerian, Jr., K. Chance, L. H. Coudert, V. Dana, V. M. Devi, J.-M. Flaud, R. R. Gamache, A. Goldman, J.-M. Hartmann, K. W. Jucks, A. G. Maki, J.-Y. Mandin, S. T. Massie, J. Orphal, A. Perrin, C. P. Rinsland, M. A. H. Smith, J. Tennyson, R. N. Tolchenov, R. A. Toth, J. Vander Auwera, P. Varanasi, and G. Wagner, *J. Quant. Spectrosc. Radiat. Transfer* **96**, 139 (2005).
12. Q. Wang, J. Wang, L. Li, and Q. Yu, *Sens. Actuators B* **153**, 214 (2011).
13. E. D. McNaghten, K. A. Grant, A. M. Parkes, and P. A. Martin, *Appl. Phys. B* **107**, 861 (2012).
14. J. Li, X. Gao, W. Li, Z. Cao, L. Deng, W. Zhao, M. Huang, and W. Zhang, *Spectrochim. Acta A* **64**, 338 (2006).
15. J. Wang, W. Zhang, L. Liang, and Q. Yu, *Sens. Actuators B* **160**, 1268 (2011).